Heliyon 10 (2024) e34010

Contents lists available at ScienceDirect

Heliyon

journal homepage: www.cell.com/heliyon

Research article

# SENP2 promotes ESCC proliferation through SETDB1 deSUMOylation and enhanced fatty acid metabolism

Linyi Sun, MSc [a,b,1], Ke Ma, MD [a,b,1], Shaoyuan Zhang, MD [a,b,1], Jianmin Gu, MD [a,b], Hao Wang, MD [a,b,**], Lijie Tan, MD [a,b,*]

[a] Department of Thoracic Surgery, Zhongshan Hospital, Fudan University, Shanghai, 200032, China
[b] Cancer Center, Zhongshan Hospital, Fudan University, Shanghai, 200032, China

ARTICLE INFO

*Keywords:*
Esophageal squamous cell carcinoma
SENP2
Proliferation
Metabolic reprogramming

ABSTRACT

Esophageal squamous cell carcinoma (ESCC) has a poor prognosis, and its metabolic reprogramming mechanism remains unclear. Small ubiquitin-like modifier(SUMO) -specific protease (SENP2) is highly related to fatty acids metabolism in some normal tissue. Thus, this study investigates the correlation between SENP2 and ESCC, and the possible mechanism. SENP2 expression was up-regulated in ESCC tissues compared to normal tissues, with high levels associated with poor overall survival rates. Knockdown of SENP2 inhibited ESCC proliferation, fatty acid uptake, and oxidation *in vitro*. RNA-seq indicated that SENP2 upregulated PPARγ, CPT1A, ACSL1, and CD36, through the deSUMOylation of SETDB1. SENP2 promotes ESCC proliferation and enhances fatty acid uptake and oxidation. High expression of SENP2 may be a poor prognostic biomarker for ESCC patients.

## 1. Introduction

Esophageal cancer is now the seventh most common cancer worldwide, reaching over 600 thousand new cases and causing over 500 thousand death in 2020 alone [1]. Esophageal squamous cell carcinoma (ESCC), with a high incidence in East Asian countries, especially China [2], has unique regional characteristics. Although comprehensive treatment has improved the prognosis for ESCC patients, the overall 5-year survival rate remains low [3]. As a result, identifying new biomarkers and treatment targets for ESCC is critical.

SUMOylation is an important post-translational modification that modulates various biological processes, including transcription [4,5], translation [6], localization [7], stability [8], and enzymatic activity [9]. The human sentrin-specific protease (SENP) family is the most extensively studied family of enzymes involved in SUMO regulation. These SENP family members are crucial to maintain the homeostasis of intracellular SUMOylation by regulating the levels of SUMO-conjugated proteins. It has been found in a pan-cancer study re-analyzing The Cancer Genome Atlas (TCGA) data that the SENP family members, are essential regulators of cancer

* Corresponding author. Department of Thoracic Surgery, Zhongshan Hospital, Fudan University Cancer Center, Zhongshan Hospital, Fudan University No 180, Fenglin Rd, Xuhui District, Shanghai, 200032, China.
** Corresponding author. Department of Thoracic Surgery, Zhongshan Hospital, Fudan University, Cancer Center, Zhongshan Hospital, Fudan University, No 180, Fenglin Rd, Xuhui District, Shanghai, 200032, China.
*E-mail addresses:* wanghao6611@163.com (H. Wang), tan.lijie@zs-hospital.sh.cn (L. Tan).
[1] Contributed equally to the work.

https://doi.org/10.1016/j.heliyon.2024.e34010
Received 27 April 2023; Received in revised form 30 June 2024; Accepted 2 July 2024
Available online 2 July 2024

**Abbreviation**

| | |
|---|---|
| ACSL1 | acyl-CoA synthetase long-chain family member 1 |
| CPT1A | carnitine palmitoyltransferase 1A |
| ESCC | esophageal squamous cell carcinoma |
| FAO | fatty acid oxidation |
| FCCP | carbonyl cyanide-*p*-trifluoromethoxyphenylhydrazone |
| FPKM | fragments per kilobase of exon per million mapped fragments |
| OCR | oxygen consumption rate |
| PCNA | proliferating pell nuclear antigen |
| PPAR-γ: | peroxisome proliferator-activated receptor gamma |
| PTM | post-translational modification |
| SENP2 | small ubiquitin-like modifier (SUMO)-specific protease 2 |
| SETDB1 | SET domain bifurcated 1 |
| TCGA | The Cancer Genome Atlas |
| 4-NQO | 4-Nitroquinoline N-oxide |

etiology, including esophageal cancer [10].

In addition, metabolic reprogramming is a prominent characteristic of tumor cells, which involves alterations in metabolic pathways during proliferation and progression [11]. Tumor cells exhibit metabolic heterogeneity by up-regulating fatty acid or amino acid metabolism [12–15]. It has been shown that ESCC tissue contains much more free fatty acids (FFA) than normal tissue [16]. However, the mechanism of this metabolic reprogramming in ESCC remains unclear.

Multiple studies have demonstrated in recent years that SENP2 plays a crucial role in regulating fatty acid metabolism. It suppresses Necdin expression by deSUMOylating cAMP response element-binding protein, thereby contributing to the formation of white and brown adipose tissue [17]. Moreover, by controlling the SUMOylation of SET domain bifurcated 1 (SETDB1), it modulates the activity of transcriptional factors, ultimately influencing the expression of peroxisome proliferator-activated receptors γ (PPARγ) [18]. In this study, we aimed to investigate whether SENP2 is involved in the ESCC etiology. We found and elucidate the involvement of SENP2 in lipid metabolism reprogramming in ESCC, and evaluate its potential as a biomarker for targeting therapy and prognosis prediction.

## 2. Methods

### 2.1. Patients and samples

We enrolled 100 patients with ESCC who underwent surgery at Zhongshan Hospital, Fudan University between January 2015 and January 2019. All patients were over 18 years old, including 77 male and 23 female patients. All patients underwent PET/CT scans to confirm the absence of distant metastasis and none of them received neoadjuvant therapy before surgery. Patients underwent surgery with negative resection margins (pR0), and the pathological diagnosis and staging were confirmed by two pathologists according to the 8th edition of the AJCC/UICC staging classification. The present retrospective study was approved by the Ethics Committee of Zhongshan Hospital, Fudan University (B2022-271R), and all patients provided informed consent for the donation of clinicobiological information and specimens.

### 2.2. Gene expression of ESCC patients from TCGA database

The fragments per kilobase of exon per million mapped reads (FPKM) gene expression data for ESCC and normal tissues including 286 healthy controls and 182 ESCC patients, were downloaded from TCGA database and GTEx database. The expression levels of SENP2 in cancer tissues and normal tissues were analyzed using a *t*-test.

### 2.3. Reverse transcription quantitative real-time PCR (RT-qPCR)

Total RNA was extracted from cells or tissues using TRIzol (Invitrogen, USA). HiScript III RT SuperMix for qPCR Kit (Vazyme, China) was used to synthesize cDNA template, and qPCR was conducted with ChamQ Universal SYBR qPCR Master Mix (Vazyme, China) in an Applied Biosystems 7300 (Thermo Fisher Scientific, USA). Relative quantification of mRNA was carried out using the $2^{-\Delta\Delta CT}$ method, with GAPDH serving as the endogenous control. Primer sequences used for qRT-PCR are shown in Supplementary Table 1.

### 2.4. Western blot analysis

Total proteins of cells or tissues were extracted using RIPA buffer (Beyotime, China) supplemented with a cocktail of protease (Selleck, China), phosphatase inhibitors (Selleck, China), and 20 mM N-ethylmaleimide (Sigma, USA). Whole cell proteins were

separated by SDS-PAGE according to molecular weight, and transferred onto PVDF membranes (0.45 μm, Merck Millipore, USA). After blocking with 5 % nofat milk, the membranes were incubated with primary antibodies, followed by incubation with an appropriate secondary antibody. Information for all antibodies is shown in Supplementary Table 2.

### 2.5. Immunohistochemical staining

The tissue samples were embedded in paraffin and cut into thin sections. The sections were deparaffinized, rehydrated, and subjected to antigen retrieval using sodium citrate buffer (pH 6.0) for 15 min. Subsequently, a hydrogen peroxide was employed to block the endogenous peroxidase activity. Following that, the tissue sections were incubated with primary antibodies at 4 °C overnight, followed by incubation with appropriate secondary antibodies. Finally, the tissue sections were counterstained with haematoxylin. Information for all antibodies is shown in Supplementary Table 2. The IHC results were evaluated by two experienced pathologists, and the patients' information was blinded to the two experts. High-density staining was defined as high SENP2 expression, and low-density staining was defined as low SENP2 expression.

### 2.6. Cell lines and cell culture

TE-1, EC109, and KYSE150 (human ESCC cell lines) were purchased from the Type Culture Collection of the Chinese Academy of Sciences (Shanghai, China). According to the cell line authentication, the STR analysis results of three cell lines matched with the STR data from the China Infrastructure of Cell Line Resources database. All the cells were cultured in RPMI-1640 medium (Gibco, USA) supplemented with 10 % fetal bovine serum and appropriate antibiotics. All the cells were placed in a constant temperature incubator at 37 °C with 5 % $CO_2$ and 95 % air.

### 2.7. Plasmid transfection and lentivira infection

Lentivira packaging was conducted in HEK-293T cells, which were stably respectively transfected with pLenti-shNC (scramble sequence), pLenti-SENP2 shRNA1 (targeted sequence: 5′-CATGCTGAAACTGGGTAATAA-3′), pLenti-SENP2 shRNA2 (targeted sequence: 5′-ATAATGGGCAGTGGTCATTTA-3′), pLV-SENP2, pLenti-SETDB1 shRNA (targeted sequence: 5′- ATGTGAGTGGATCTAT CG-3′) and contransfected with lentivira packaging plasmids. The lentivira solution was collected from cell culture medium after 48 h and filtered through a 0.45 μm filter. TE-1 cells and KYSE150 cells were infected with pLenti-shNC or pLenti-SENP2 shRNA1 or pLenti-SENP2 shRNA2 lentivira solution to construct shNC TE-1 cells, SENP2 sh1 TE-1 cells and SENP2 sh2 TE-1 cells, while EC109 cells were infected with pLV-SENP2 to construct the OE SENP2 EC109 cells. As for transient transfection, cells were transfected with Flag-SETDB1 WT, Flag-SETDB1 KR (K1050R), HA-SUMO2, Myc-SENP2, Myc-SENP2 mut (C548S), HA-CD36. SETDB1 siRNA and scramble siRNA were transfected into TE-1 cells to knockdown the expression of endogenous SETDB1. All plasmids transfections were performed with liposomal transfection reagent (Yeasen Biotech, China). The plasmids including HA-SUMO2, Myc-SENP2, Myc-SENP2 mut (C548S), Flag-SETDB1 WT, Flag-SETDB1 KR (K1050R), SETDB1 siRNA and scramble siRNA were gifts from Quan Zheng (Shanghai Jiao Tong University School of Medicine, Shanghai, China) [18]. pLenti-shNC, pLenti-SENP2 shRNA1, pLenti-SENP2 shRNA2, pLV-SENP2, pLenti-SETDB1 shRNA, HA-CD36 plasmids were purchased from Tsingke Biotechnology (Shanghai, China).

### 2.8. Cell Counting Kit-8 assay

Cells were seeded in 96-well culture plates at a density of 2000 cells per well and were cultured for 0, 6, 24, 48, and 72 h. At each time point, 10 μl Cell Counting Kit-8 reagent (Yeasen Biotechnology, Shanghai, China) was added to each well. Then the plates were incubated in the dark for 1 h at 37 °C. Finally, the absorbance value of each well was detected at 450 nm.

### 2.9. EdU staining

EdU staining was conducted using the BeyoClick™ EdU Cell Proliferation Kit with Alexa Fluor 594 (Beyotime, China). When the cell density reached about 50 %, EdU was added to the cell culture dish to a final concentration of 10 μM (1X). After incubation for 2 h, the culture medium was removed, and 1 ml of 4 % paraformaldehyde (PFA) was added for 15 min at room temperature. The reaction mixture was prepared according to the instructions and added to cells, followed by incubation for 30 min at room temperature in the dark. To stain cell nuclei, cells were incubated with Hoechst 33342 for 10 min at room temperature in the dark.

### 2.10. Wound healing assay

Cells were seeded into six-well culture plates and cultured until reaching 90 % confluence. Horizontal scratch of approximately 0.5 cm wide was made across the cell layer. Photographs were taken at 0, 12 and 24 h to record the width of the scratch. The cell migration rate was analyzed using ImageJ software (National Institutes of Health, Bethesda, MD, USA).

### 2.11. Transwell migration assay

600 μl RPMI-1640 medium containing 10 % fetal bovine serum was added into each lower chamber of the 24-well culture plate,

and $4 \times 10^4$ cells (200 μl without fetal bovine serum) were seeded in the upper chamber of the Transwell inserts (Corning Inc., Corning, NY, USA). Cells were incubated for 18–24 h. After removing the medium, 4 % PFA was added into the lower chamber and then the cells were stained with 0.1 % crystalline violet. Count the cells on the bottom surface of the chamber using an inverted microscope.

### 2.12. Apoptosis assay

Cells ($1 \times 10^5$) were collected and resuspended in 100 μl of 1 × binding buffer. Then cells were stained with 5 μl of Annexin V and 10 μl of 7-AAD (Yeasen Biotechnology, Shanghai, China) in the dark for 15min. After compensating for untreated cells, fluorescence cells were analyzed via fluorescence-activated cell sorting (Beckman-Coulter, CA, USA).

### 2.13. Detection of long chain fatty acid oxidation and ATP levels

A long-chain fatty acid oxidation stress test was performed by Seahorse XF Palmitate Oxidation Stress Test Kit (Seahorse Bioscience, Agilent) and was evaluated through the Seahorse XFe24 analyzer. Etomoxir (4 μM final concentration), oligomycin (5 μM final concentration), Carbonyl cyanide-*p*-trifluoromethoxyphenylhydrazone (FCCP) (optimal concentration: 0 μM final to 2.0 μM final), and antimycin A/rotenone (Rote + AA; 0.5 μM final concentration) were added in that order. ATP levels were detected using Enhanced ATP Assay Kit (S0027, Beyotime, Shanghai, China) according to the manufacturer's instructions.

### 2.14. NAD+/NADH measurement and NADP+/NADPH measurement

The ratio of NAD+/NADH and NADP+/NADPH were respectively measured using commercial NAD+/NADH Assay Kit with WST-8 (Beyotime, China) and NADP+/NADPH Assay Kit with WST-8 (Beyotime, China), according to the manufacturer's protocols. In brief, cells were washed with cold PBS, lysed with 200 μl of NAD/NADH extraction buffer, and centrifuged at 13,000×*g* for 5 min at 4 °C. The supernatant was then divided into two aliquots for total NAD detection (or total NADP detection) and NAD decomposition (or NADP decomposition) at 60 °C for 30 min. The samples were then transferred to a 96-well plate, and the absorbance at 450 nm was measured. The amount of NAD+ (or NADP+) was determined by subtracting the amount of NADH (or NADPH) from the amount of total NAD (or total NADP). The ratio of NAD/NADH was determined by the following equation: NAD/NADH = (NADtotal – NADH)/NADH. The ratio of NADP/NADPH was determined by the following equation: NADP/NADPH = (NADPtotal – NADPH)/NADPH.

### 2.15. Fatty acid uptake assay

When the cell density reached about 50 %, BODIPY® FL C12 (Thermo Scientific, USA) was added into each well at a final concentration of 2 μM for 15 min at 37 °C. Cells ($1 \times 10^5$) were collected and resuspended in 100 μl of 1 × binding buffer. After compensating for untreated cells, fluorescence cells were analyzed via fluorescence-activated cell sorting (Beckman-Coulter, CA, USA).

### 2.16. RNA-seq and bioinformatic analysis

Total RNA was extracted from SENP2 knockdown TE-1 cells and negative control TE-1 cells using TRIzol reagent (Invitrogen, USA). Sequencing and preliminary analysis were conducted at Sangon Biotech (Shanghai, China) to identify differentially expressed genes (DEGs), which were subsequently classified according to the Kyoto Encyclopedia of Genes and Genomes (KEGG) database and Gene Ontology (GO) database.

### 2.17. Immunoprecipitation

The cell lysate was obtained as described above. Primary antibodies and protein A/G beads or Flag-beads were added to the cell lysate to enrich specific proteins, and the proteins were then eluted from the beads. The proteins were detected by Western blot analysis as described above. Information for all antibodies is shown in Supplementary Table 2.

### 2.18. Animal experiments

All animal experiments were approved by the Animal Ethics Committee of Shanghai Jiaotong University School of Medicine. Six-week-old C57BL/6 female mice were purchased from Shanghai JieSiJie Experimental Animal Co., Ltd. The esophageal spontaneous squamous cell carcinoma model was constructed. The mice were fed with distilled water containing 4-Nitroquinoline N-oxide (4-NQO) (100 mg/L) for 16 weeks, and then fed normal distilled water for 12 weeks. The mice were harvested at 28 weeks and the esophagi were collected for further analysis. The BALB/C female nude mice were purchased from Shanghai JieSiJie Experimental Animal Co., Ltd. Eighteen female mice (five weeks old) were randomly divided into three groups (n = 6/group) according to body weight: shNC group, SENP2 sh1 group, and SENP2 sh2 group. Transfected cells ($5 \times 10^6$) were subcutaneously injected into the right armpit of each mouse. Tumor volume was calculated every three days. At 21 days after inoculation, the mice were euthanized by cervical dislocation. The final weight was measured, and the tumour volume was calculated using the following formula: volume = (length × width$^2$)/2.

### 2.19. Statistical analysis

Statistical analyses were performed with SPSS version 26 (IBM, Chicago, IL, USA), GraphPad (Version 9.3, GraphPad Software, San Diego, CA, USA), and R software (Version 4.3.0, R Foundation for Statistical Computing, Vienna, Austria). Baseline features were analyzed by the "tableone" package in R software. The clinicopathological parameters of the patients were compared using the Kruskal–Wallis test and $\chi^2$ test. Kaplan–Meier analysis was used to determine the relationships between SENP2 expression and overall survival rate and recurrence-free survival rate according to the log-rank test. An unpaired *t*-test was used to compare the relative data between NC group and SENP2 overexpression group. One-way ANOVA was used to compare differences between multiple groups.

## 3. Result

### 3.1. SENP2 is significantly elevated in ESCC tissue

To explore the expression level of SENP2, the gene expression data of ESCC tissue (n = 182) and normal esophageal tissue (n = 286) were exported from the TCGA database and GTEx database. Compared to normal tissues, SENP2 expression was significantly increased in esophageal squamous cell carcinoma tissues (Fig. 1A). To validate these results, the mRNA and protein levels of SENP2 were detected in postoperative cancer tissues and distant normal epithelial tissues from ESCC patients, and the results indicated that both SENP2 mRNA and protein levels were increased in tumor tissues (Fig. 1B and C). Moreover, SENP2 was also significantly upregulated in tumor tissues obtained from the spontaneous ESCC mouse model compared to normal esophageal epithelial tissues (Fig. 1D and E).

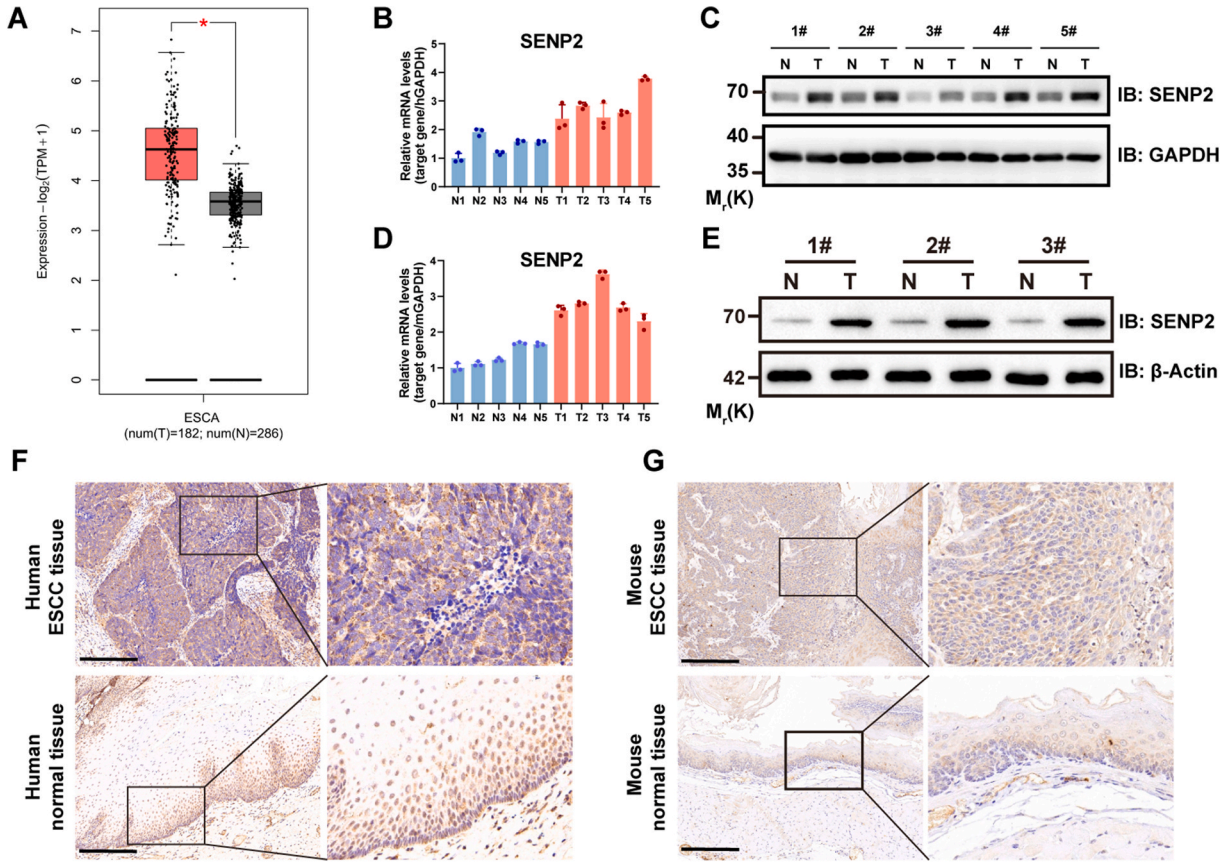


**Fig. 1.** *SENP2 is elevated in human and mouse ESCC tissues.*
**(A)** Expression levels of SENP2 in ESCC tissues (n = 182) and unpaired normal esophageal squamous epithelium tissues (n = 286) in The Cancer Genome Atlas database and Genotype-Tissue Expression database. *P < 0.01. **(B–C)** Both SENP2 mRNA and protein level in ESCC tissue and normal esophageal squamous epithelium, were respectively measured by qRT-PCR and Western blot. The tissue was collected immediately after surgery from ESCC patients. This image was published with the patient's consent. **(D–E)** SENP2 mRNA and protein level in mouse ESCC tissue and normal esophageal squamous epithelium. The tissue was collected from mice after 4-NQO treatment. **(F–G)** Representative images of SENP2 staining in the IHC assay. the SENP2 expression in human ESCC tissues and mouse ESCC tissues, especially in cancer nests, was higher than that in normal esophageal epithelium. Scale bar: 200 μm. Data are presented as the means ± SD. Non-adjusted images of blots are shown in Supplementary Material 1.

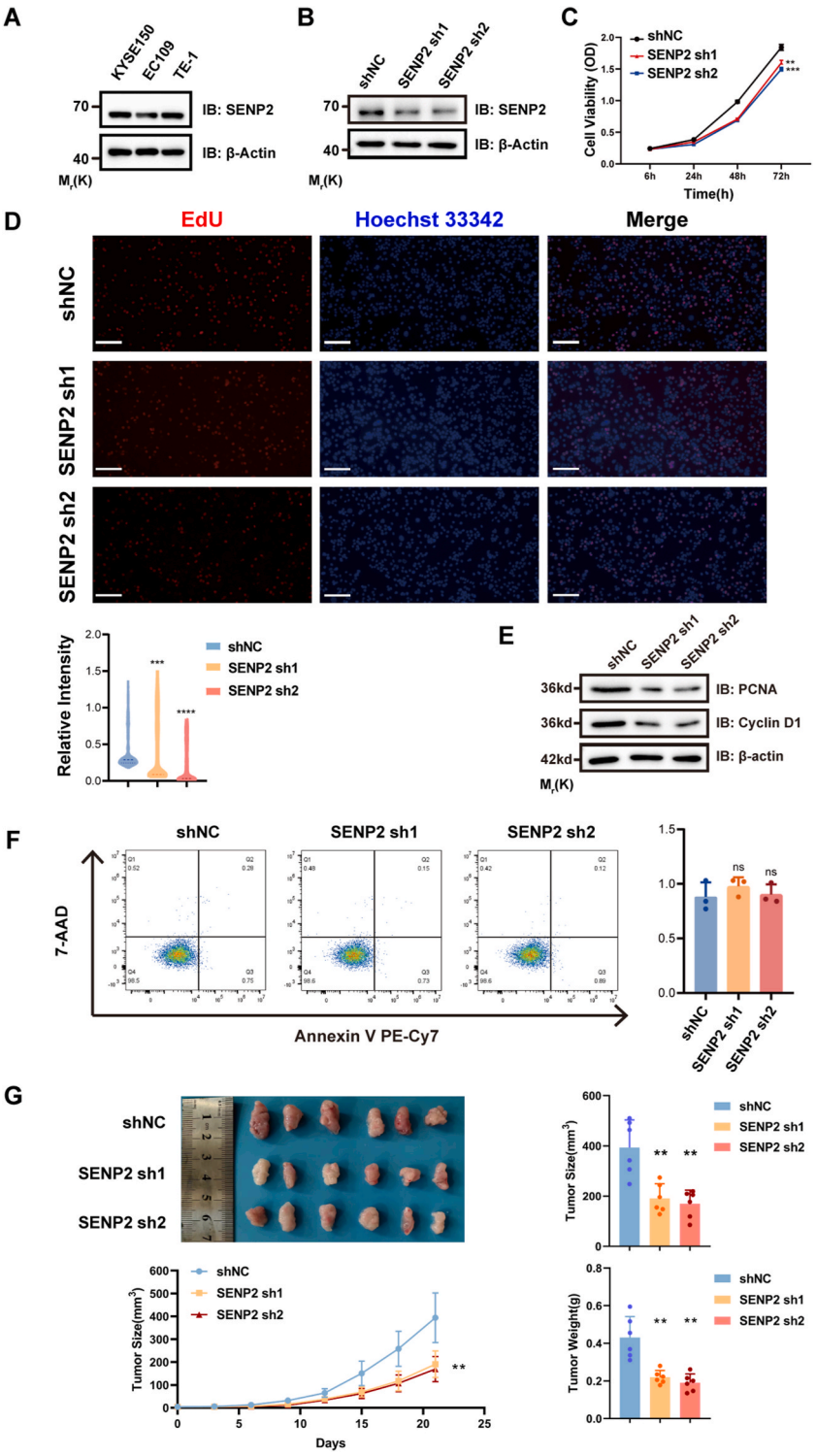


*(caption on next page)*

**Fig. 2.** *SENP2 promotes the proliferation of ESCC cells*
**(A)** SENP2 expression levels in three ESCC cell lines were detected by Western blot assay. **(B)** SENP2 expression levels were detected by Western blot assay in shNC, SENP2 sh1 TE-1 cells, and SENP2 sh2 TE-1 cells. **(C)** Cell proliferation was measured by a CCK-8 assay in shNC, SENP2 sh1, SENP2 sh2 TE-1 cells. $^{**}P < 0.01$, $^{***}P < 0.001$ **(D)** Representative images of EdU staining in shNC, SENP2 sh1 and SENP2 sh2 TE-1 cells. Scale bar: 200 μm. Histogram shows that downregulated SENP2 expression inhibits cell proliferation. $^{***}P < 0.001$ $^{****}P < 0.0001$ **(E)** The expression of PCNA and Cyclin D1 in shNC, SENP2 sh1 and SENP2 sh2 TE-1 cells. **(F)** Representative images of the cell apoptosis analysis by Annexin V/7-AAD staining. ns: not significant, $P > 0.05$. **(G)** After inoculation, the tumor volume was measured every three days and growth curve of subcutaneous ESCC models was drawn. 21 days after inoculation, the tumor volumes and weights was measured after the mice were euthanized. $^{**}P < 0.01$. Data are presented as the means ± SD. Non-adjusted images of blots are shown in Supplementary Material 2.

Furthermore, through immunohistochemical staining, the expression of SENP2 in human esophageal cancer tissues and mouse esophageal cancer tissues, especially in cancer nests, was higher than that in normal esophageal epithelial tissues (Fig. 1F and G).

### 3.2. SENP2 enhances the proliferation of ESCC cells

To explore the role of SENP2 in the development of ESCC, SENP2 knockdown cell lines were generated by two different SENP2 shRNA from TE-1 and KYSE150 cell lines with relatively high expression of SENP2 (Fig. 2A and B, Supplementary Fig. 1A). Meanwhile, a SENP2 overexpression cell line were generated from EC109 cell line (Supplementary Fig. 1A). CCK-8 and EdU staining assays

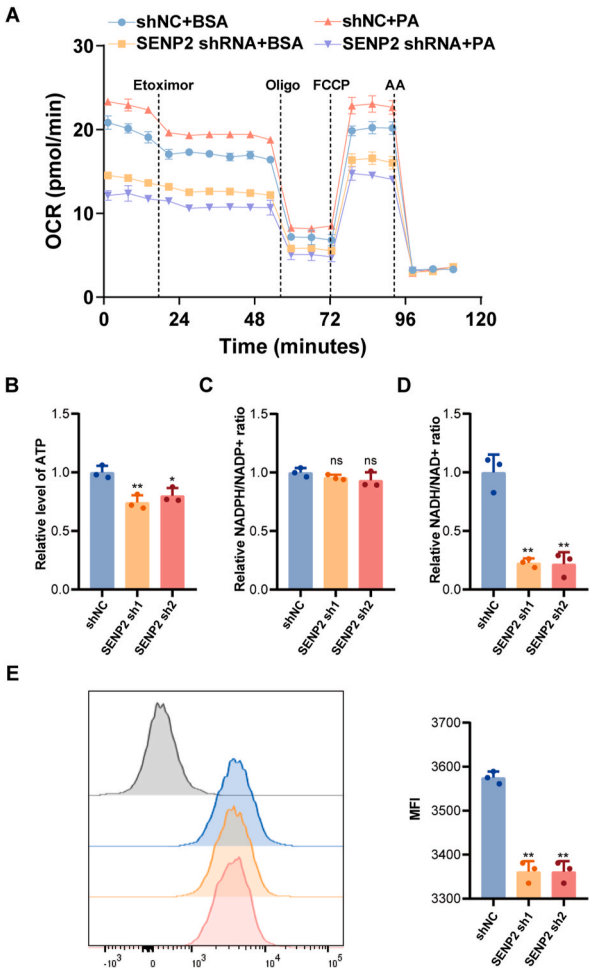


**Fig. 3.** *SENP2 deficiency diminishes the fatty acid uptake and fatty acid oxidation.*
**(A)** PA-dependent OCR curve from SENP2 sh1 or shNC TE-1 cell lines. **(B)** ATP production was detected using a luciferase-based assay in shNC, SENP2 sh1 and SENP2 sh2 TE-1 cells. $^{*}P < 0.05$, $^{**}P < 0.01$. **(C–D)** The ratio of NADH/NAD+ and NADPH/NADP+ were measured in shNC, SENP2 sh1 and SENP2 sh2 TE-1 cells. $^{**}P < 0.01$, ns: not significant, $P > 0.05$. **(E)** The ability of fatty acid uptake of TE-1 cell lines was evaluated through incubated in RPMI medium containing BODIPY® FL C12 with or without knockdown of SENP2. Histogram depicted the quantitative analysis of relative Bodipy-C12 intensity. $^{**}P < 0.01$. Data are presented as the means ± SD. Non-adjusted images of blots are shown in Supplementary Material 3.

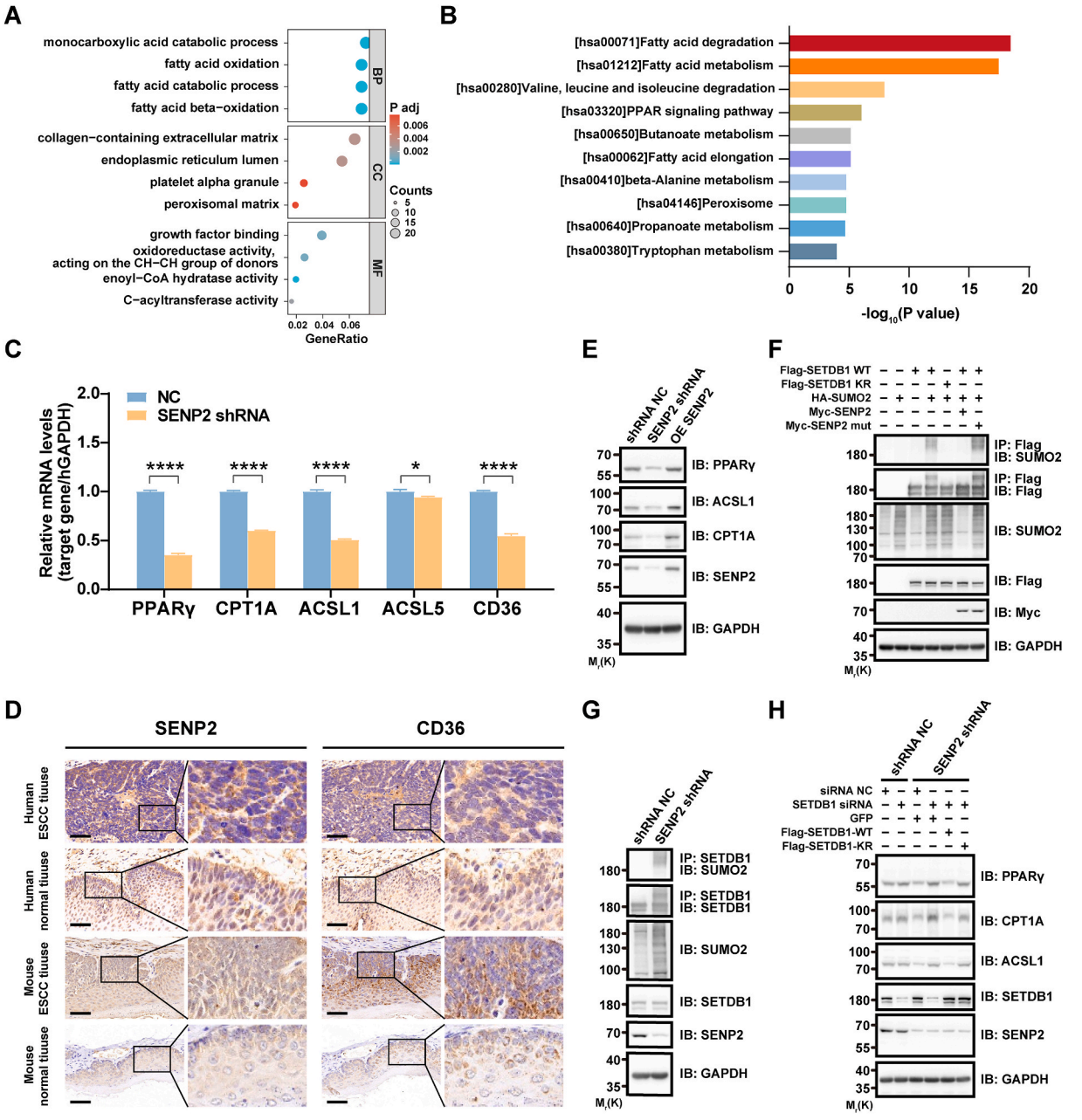


**Fig. 4.** *Knockdown of SENP2 inhibits the expression of proteins related to lipid metabolism through deSUMOylation of SETDB1.*
**(A)** The graph represented GO functional enrichment analyses of DEGs in TE-1 cell lines with or without SENP2 knockdown. **(B)** Comparison of DEGs in TE-1 cell lines with or without SENP2 knockdown was analyzed by KEGG Pathway analysis. **(C)** The expressions of fatty acid metabolic DEGs were detected in SENP2 knockdown or shNC TE-1 cell lines by qRT-PCR. $*P = 0.0150$, $****P < 0.0001$. **(D)** Representative images of SENP2 staining and CD36 staining in the IHC assay. The expression of SENP2 and CD36 were both higher in ESCC tissue than those in normal tissue. Scale bar: 100 μm. **(E)** The expression levels of PPARγ, ACSL1, and CPT1A in shNC, shSENP2 TE-1 cells, and shSENP2 TE-1 cells which were transfected with Flag-SENP2. **(F)** HEK-293T cells were cotransfected with Flag-SETDB1, HA-SUMO2 to verify the SUMOylation of SETDB1. Then the cells were transfected with Myc-SENP2, or Myc-SENP2mut (C548S) to confirm that SENP2 deSUMOylated SETDB1. Anti-Flag beads were used to concentrate SETDB1 as well as its binding protein. **(G)** The cell lysates from shNC TE-1 cells or shSENP2 TE-1 cells were immunoprecipitated with anti-SETDB1 antibody and then immunoblotted with anti-SETDB1 and anti-SUMO2 antibody. **(H)** TE-1 shNC and shSENP2 cells were transfected with SETDB1 siRNA to knockdown endogenous SETDB1, and then transfected with SETDB1-WT or SETDB1-K1050R. Scramble siRNA and GFP served as the negative control. These cells were lysed and immunoblotted with anti-PPARγ, anti-CPT1A, anti-ACSL1, anti-SETDB1, anti-SENP2, or anti-GAPDH antibodies. Data are presented as the means ± SD. Non-adjusted images of blots are shown in Supplementary Material 4.

revealed that the proliferation of SENP2-deficient ESCC cells was significantly suppressed, while the proliferation of ESCC cells was promoted by SENP2 overexpressing. (Fig. 2C and D, Supplementary Figs. 1C and 1E). To exclude the influence of apoptosis, cells were stained with Annexin V and 7-AAD, which demonstrated that the proportions of apoptotic and necrotic cells did not significantly change regardless of the expression level of SENP2. (Fig. 2F, Supplementary Fig. 1D). Moreover, the expression of PCNA and Cyclin D1, key regulators of the cell cycle, was inhibited by SENP2 knockdown, confirming that SENP2 plays an important role in tumour proliferation (Fig. 2E, Supplementary Fig. 1B). However, Transwell and wound-healing assays showed that SENP2 had no significant effect on the migration ability of ESCC cells (Supplementary Figs. 2A and 2B). Moreover, subcutaneous tumorigenic assays confirmed that low SENP2 expression led to a decrease in both size and weight of tumors, further supporting the positive impact of SENP2 on tumor development (Fig. 2G). These results revealed that the tumorigenic ability of ESCC cells is weakened after SENP2 knockdown and upregulating the expression of SENP2 could enhances the proliferation of ESCC cells.

*3.2.1. SENP2 regulates lipid metabolism reprogramming in ESCC and increases energy production*

Because SENP2 plays a vital role in adipocytes, hepatocytes, and skeletal muscle cells [17–19], the present study investigated whether SENP2 is also involved in ESCC fatty acid metabolism to influence the energy supply. The oxygen consumption rate of the control group decreased after the addition of etomoxir (Carnitine Palmitoyltransferase 1A inhibitor, CPT1A inhibitor), whereas inhibiting the expression of SENP2 downregulated the overall OCR, as etomoxir had little effect on the OCR, which indicated that inhibiting SENP2 played a similar role to etomoxir to some extent. Moreover, when palmitic acid was added as the substrate for oxidation, the OCR was slightly increased in both the NC group and SENP2 knockdown group (Fig. 3A). Futhermore, the ATP content decreased when the expression of SENP2 was suppressed (Fig. 3B). Furthermore, we detected the ratios of NADH/NAD+ and NADPH/NADP+ in the cells of the three groups, and found that NADH/NAD + ratio but not NADPH/NADP + ratio was significantly decreased in SENP2-deficient TE-1 cells (Fig. 3C and D), which indicated less NADH was generated to support energy metabolism.

Fluorescently labelled BODIPY FL C12, as a long-chain fatty acid analogue was used to investigate lipid trafficking, which demonstrated that the uptake of long-chain fatty acids was significantly reduced in SENP2-deficient cells (Fig. 3E). Together, these findings suggested that SENP2 may accelerate the uptake of fatty acids in ESCC cells and promote fatty acid oxidation to generate energy for cell proliferation.

SENP2 regulates the expression of key enzymes involved in lipid metabolism by modulating the SUMOylation of SETDB1.

To further explore the mechanism by which SENP2 regulates lipid metabolism in ESCC, RNA-seq assays were performed on SENP2-knockdown and wild-type ESCC cells. GO enrichment and KEGG analyses indicated that the differentially expressed genes (DEGs) were significantly enriched in the fatty acid oxidation pathway, fatty acid degradation pathway and PPAR signaling pathway (Fig. 4A and B). According to the RNA-seq results, the expression levels of five DEGs that were related to fatty acid metabolism and had the largest fold change were validated by qRT−PCR, WB, or IHC. PPARγ, CPT1A, acyl-CoA synthetase long-chain family member 1 (ACSL1), and CD36 were significantly suppressed when SENP2 was downregulated (Fig. 4C-E). Furthermore, energy production increased significantly after overexpressing CD36 in SENP2-deficient cells (Supplementary Figs. 3A and 3B). These results suggested that SENP2 may regulate lipid metabolism in ESCC by modulating genes involved in lipid trafficking and fatty acid oxidation.

As found in previous work [18], in adipocytes, SENP2 promotes the transcription of PPARγ and CD36 mainly through SETDB1 deSUMOylation. Therefore, the present study investigated whether this mechanism of SENP2 plays the same role in the regulation of

**Table 1**
Correlation analysis between the expression of SENP2 and clinicopathological parameters in ESCC patients.

| Variables | SENP2 expression | | *P* value[a] | All cases (n = 100) |
|---|---|---|---|---|
| | Low (n = 43) | High (n = 57) | | |
| Age (median [IQR]) | 65.0 [58.0, 69.0] | 65.0 [59.0, 68.0] | 0.986 | 65.0 [58.0, 69.0] |
| Gender (%) | | | 0.997 | |
| Female | 10 (23.3) | 13 (22.8) | | 23 (23.0) |
| Male | 33 (76.7) | 44 (77.2) | | 77 (77.0) |
| Differentiation (%) | | | 0.239 | |
| 1 | 2 (4.7) | 0 (0.0) | | 2 (2.0) |
| 2 | 25 (58.1) | 37 (64.9) | | 62 (62.0) |
| 3 | 16 (37.2) | 20 (35.1) | | 36 (36.0) |
| pT stage (%) | | | 0.063 | |
| 1a | 3 (7.0) | 2 (3.5) | | 5 (5.0) |
| 1b | 14 (32.6) | 7 (12.3) | | 21 (21.0) |
| 2 | 7 (16.3) | 14 (24.6) | | 21 (21.0) |
| 3 | 19 (44.2) | 34 (59.6) | | 53 (53.0) |
| pN stage (%) | | | 0.407 | |
| 0 | 25 (58.1) | 38 (66.7) | | 63 (63.0) |
| 1 | 17 (39.5) | 15 (26.3) | | 32 (32.0) |
| 2 | 1 (2.3) | 3 (5.3) | | 4 (4.0) |
| 3 | 0 (0.0) | 1 (1.8) | | 1 (1.0) |
| SUVmax (median [IQR]) | 12.5 [5.7, 16.7] | 12.70 [9.8, 16.8] | 0.531 | 12.7 [9.0, 16.9] |
| Ki-67 (%) (median [IQR]) | 60.0 [40.0, 75.0] | 60.0 [40.0, 70.0] | 0.672 | 60.0 [40.0, 70.0] |

Data are number. (%) or mean ± SD or median (IQR); pT stage: pathological T stage; pN stage: pathological N stage.
[a] *P* value for comparing clinicopathological parameters in SENP2 low-expression group versus high-expression group.

proliferation and fatty acid metabolic reprogramming in ESCC cell lines. Firstly, HEK-293T cells were cotransfected with SETDB1 WT or K1050R plasmids and SUMO2, as well as SENP2 WT or SENP2 C548S plasmids. The results confirmed that SETDB1 was SUMOylated at Lys1050, and SENP2 disrupted SUMO2 conjugation to SETDB1 via catalytic deSUMOylation (Fig. 4F). Next, SETDB1 expression and SETDB1 SUMOylation levels were detected in shNC- and shSENP2-transfected TE-1 cells. As expected, the expression of SETDB1 did not significantly change in SENP2-deficient ESCC cells, but SETDB1 SUMOylation levels significantly increased (Fig. 4G), Futhermore, the expression of SETDB1 are similar in both cancer and normal tissues regardless of the expression level of SENP2 (Supplementary Fig. 3C). Then we inhibited the endogenous SETDB1 in both shNC and shSENP2 TE-1 cells and tranfected the cells with either SETDB1 WT or KR plasmid, respectively. It turned out that CPT1A, PPARγ, and ACSL1 levels were downregulated in SENP2-deficient cells but not in SETDB1-deficient cells. In addition, the downregulation of those metabolic-related proteins was reversed if SETDB1 lost the SUMO conjugation site (Fig. 4H). Subsequently, the cell proliferation and apoptosis were detected to investigate the role of SUMOylation of SETDB1 in ESCC cells. There was no significant impact on the proliferation ability of ESCC cells when knocking down SETDB1 alone, or knocking down SETDB1 and SENP2 simultaneously. However, with knockdown of both SENP2 and SETDB1, overexpressing SETDB1-WT but not SETDB1-KR inhibited the cell growth (Supplementary Fig. 3D). Besides, there were no significant difference in the proportion of apoptotic and necrotic cells among those cell lines (Supplementary Fig. 3E). Therefore, these findings suggested that high SENP2 expression in ESCC negatively modulates the SUMOylation of SETDB1, thereby promoting the expression of downstream genes related to fatty acid metabolism.

### 3.3. *SENP2 expression in ESCC tissue is related to patient prognosis*

Given that SENP2 plays a vital role in the lipid metabolism and proliferation in ESCC, the ability of SENP2 to predict the prognosis of ESCC patients was investigated. One hundred ESCC patients who underwent surgery at Zhongshan Hospital, Fudan University were enrolled in this study. Postoperative tumor specimens were obtained for tissue arrays analysis. The detailed baseline clinicopathological characteristics of 100 patients are presented in Table 1. The expression of SENP2 in tumor tissues of each patient was detected by IHC and analyzed by two experienced pathologists. Among the 100 patients with ESCC, 43 patients had low SENP2 expression, and 57 patients had high SENP2 expression. There were no significant differences in age, gender, pathological differentiation grades,or pathological N stages between the high-intensity and low-intensity groups. Of note, high SENP2 expression may have led to a poor pathological T stage, but there was no statistical significance ($P = 0.063$). In addition, primary tumor SUVmax ([9.80, 16.80] vs [5.70, 16.73], $P = 0.531$) was slightly higher in the high SENP2 expression group, though this difference was not significantly different. Moreover, patients with relatively high SENP2 expression had worse overall survival (HR = 2.040, $P = 0.040$) and recurrence-free survival (HR = 0.466, $P = 0.017$) than patients with low SENP2 expression, the Kaplan-Meier curve was shown in (Fig. 5A,B).

## 4. Discussion

Esophageal squamous cell carcinoma is one of the most common tumors in East Asian countries [2]. However, there is a lack of specific driver genes that can serve as biomarkers for early diagnosis or targeted therapy. Currently, an increasing number of studies have focused on comprehensive changes in tumors, especially metabolic reprogramming, as key enzymes in lipid uptake and catabolism are often overexpressed or hyperactivated in various cancers [20–22]. This research is the first to show that SENP2, a specific deSUMOylation protease, enhances the fatty acid degradation and consumption through increasing the expression of PPARγ, CPT1A, ACSL1, and CD36 by deSUMOylating SETDB1, which generates more energy to support ESCC proliferation.

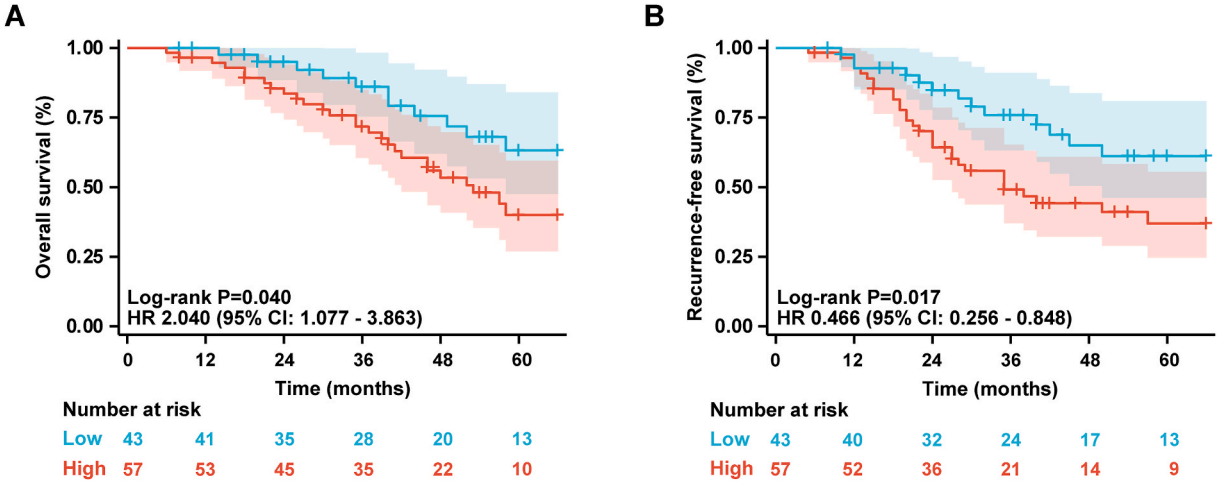


**Fig. 5.** *High level of SENP2 is related to poor prognosis in ESCC patients*
**(A)** High level of SENP2 indicates worse overall survival in patients with ESCC. HR = 2.040, $P = 0.040$. **(B)** High level of SENP2 indicates worse recurrence-free survival in patients with ESCC. HR = 0.466, $P = 0.017$. Both survival rates were quantified by Kaplan–Meier survival analysis.

Metabolic reprogramming modulates the metabolic processes of tumor cells to meet the energy necessary for their proliferation. Key enzymes involved in lipid uptake and catabolism are often aberrantly overexpressed or hyperactivated in various cancer types, thereby sustaining growth, invasion, and metastasis [23,24]. Our research revealed that SENP2 promotes tumor proliferation and fatty acid metabolism in ESCC. Previous studies have shown that the content of free fatty acids continuously increases from muscle tissue, and normal epithelial cells to cancer tissue to meet an urgent need for energys, cell membrane biosynthesis, and signal transduction [16]. CD36, a key cell membrane protein for the free fatty acid uptake, is involved in regulating the predominant metabolic preference of ESCC patients and is related to prognosis. ESCC with high CD36 expression tends to use fatty acids to promote tumor proliferation, and tumour growth is slowed down when CD36 is suppressed, while the supplement of amino acids can restore the proliferation [25]. ACSL family, which catalyses the transformation of FFAs into acyl-CoA, plays a vital role in the first step of fatty acid degradation. It has been reported that the expression of ACSL1 in ESCC tumor tissue is higher than that in normal tissue [26]. Moreover, CPT1A is the key enzyme that transfers acyl-CoA into mitochondria for β-oxidation. Tian et al. [27] reported that CPT1A overexpression maintains redox homeostasis by providing GSH and NADPH, as well as protects ESCC cells from apoptosis upon detached culture. Therefore, the present results suggested that SENP2 enhances the lipid metabolism in ESCC by up-regulating CD36, ACSL1, and CPT1A to provide more energy for proliferation. However, apoptosis was unaffected, which may have been due to culturing cells in an attached state without exposure to apoptosis-related stimuli. The present study demonstrated that the reprogramming of lipid metabolism mediated by SENP2 is important for the progression of esophageal squamous cell carcinoma, thereby warranting additional research.

SENP2 has been reported to participate in fatty acid oxidation in liver tissue [28] and skeletal muscle [19] as well as in the differentiation of adipose tissue [17], while its underlying regulatory mechanism is tissue-specific. PPARs activate the expression of their target genes by binding to peroxisome proliferator response elements (PPREs) [29]. Previous research has shown that SENP2 modulates PPARα, β, or γ to affect the expression of downstream target genes [28,30,31]. In the present study, RNA-seq data demonstrated that among the DEGs related to fatty acid metabolism, *PPARG* had the greatest fold change. According to previous reports, *CD36*, *ACSL1*, and *CPT1A* can all be target genes of PPARγ [32,33]. Therefore, it would be possible that the changes in lipid metabolic enzymes are mediated by PPARγ in ESCC, which needs to be further explored.

Previous work has revealed that SENP2 is essential for the expression of PPARγ by inhibiting the catalytic activity of SETDB1. Similarly, in the present study, the inhibition of SENP2 suppressed the expression of PPARγ, CPT1A, ACSL1, and CD36 via the SUMOylation of SETDB1 in ESCC. SETDB1 is a histone methyltransferase, that results in H3K9me2 or H3K9me3. Highly methylated histones bind more tightly to DNA, thereby suppressing DNA transcription [34]. The C-terminus of SETDB1 is the active region of methyltransferase, and the monoubiquitination modification at lysine-867 is essential for its enzymatic activity [35]. Because the SUMOylation site of SETDB1 is located at lysate-1050, which is also at the C-terminus and near the ubiquitination site, SUMOylation may affect ubiquitination. Thus, we hypothesized that when SENP2 is suppressed, the SUMOylation level of SETDB1 increases, which may enhance its methylase activity and inhibit the transcription of *PPARG*.

However, there were still several limitations that need to be clarified. Due to the heterogeneous role of SENP2 in tissues, further methods, such as immunofluorescence colocalization, are needed to determine whether SENP2 directly regulates PPARγ in ESCC. In addition, coimmunoprecipitation mass spectrometry should be used to determine whether SENP2 participates in the regulation of other metabolic processes by interacting with other proteins. Moreover, additional studies should be performed to determine whether upregulated transcriptional activity affects the expression of other cell proliferation-related genes.

## 5. Conclusion

In summary, this study demonstrated that SENP2 promotes the proliferation of ESCC by affecting lipid metabolism, which may serve as a potential biomarker for prognosis and provide a theoretical basis for individualized treatment. Metabolic inhibitors are unlikely to be effective as targeted therapies, but when combined with targeted drugs, they may improve the efficacy of targeted therapy and reduce the occurrence of drug resistance.

## Disclosure of interest

The authors have no conflicts of interest.

## Funding statement

Dr. Hao Wang was supported by the Excellent Doctor Project of Zhongshan Hospital, Fudan University, China [grant number: 2021ZSGG15].

## Data availability statement

The data used in this study are available from the corresponding author upon reasonable request. However, according to the National Biosafety Law of the People's Republic of China, specific patient information cannot be provided, and only statistical data can be displayed.

## CRediT authorship contribution statement

**Linyi Sun:** Writing – original draft, Formal analysis, Data curation, Conceptualization. **Ke Ma:** Writing – original draft, Validation, Formal analysis, Data curation, Conceptualization. **Shaoyuan Zhang:** Validation, Formal analysis, Data curation. **Jianmin Gu:** Supervision, Methodology, Data curation, Conceptualization. **Hao Wang:** Writing – review & editing, Supervision, Project administration, Funding acquisition, Conceptualization. **Lijie Tan:** Writing – review & editing, Supervision, Project administration, Methodology, Funding acquisition, Conceptualization.

## Declaration of competing interest

The authors declare that they have no known competing financial interests or personal relationships that could have appeared to influence the work reported in this paper.

## Appendix A. Supplementary data

Supplementary data to this article can be found online at https://doi.org/10.1016/j.heliyon.2024.e34010.

## References

[1] H. Sung, J. Ferlay, R.L. Siegel, et al., Global cancer statistics 2020: GLOBOCAN estimates of incidence and mortality worldwide for 36 cancers in 185 countries, CA A Cancer J. Clin. 71 (2021) 209–249.
[2] E. Morgan, I. Soerjomataram, H. Rumgay, et al., The global landscape of esophageal squamous cell carcinoma and esophageal adenocarcinoma incidence and mortality in 2020 and projections to 2040: new estimates from GLOBOCAN 2020, Gastroenterology 163 (2022).
[3] J.K. Waters, S.I. Reznik, Update on management of squamous cell esophageal cancer, Curr. Oncol. Rep. 24 (2022) 375–385.
[4] A. Nayak, A. Reck, C. Morsczeck, et al., Flightless-I governs cell fate by recruiting the SUMO isopeptidase SENP3 to distinct genes, Epigenet. Chromatin 10 (2017) 15.
[5] H.-Y. Ryu, D. Zhao, J. Li, et al., Histone sumoylation promotes Set3 histone-deacetylase complex-mediated transcriptional regulation, Nucleic Acids Res. 48 (2020) 12151–12168.
[6] C.F. de la Cruz-Herrera, M. Campagna, M.A. García, et al., Activation of the double-stranded RNA-dependent protein kinase PKR by small ubiquitin-like modifier (SUMO), J. Biol. Chem. 289 (2014) 26357–26367.
[7] X. Shangguan, J. He, Z. Ma, et al., SUMOylation controls the binding of hexokinase 2 to mitochondria and protects against prostate cancer tumorigenesis, Nat. Commun. 12 (2021) 1812.
[8] F. Lamoliatte, F.P. McManus, G. Maarifi, et al., Uncovering the SUMOylation and ubiquitylation crosstalk in human cells using sequential peptide immunopurification, Nat. Commun. 8 (2017) 14109.
[9] X.-X. Sun, Y. Chen, Y. Su, et al., SUMO protease SENP1 deSUMOylates and stabilizes c-Myc, Proc. Natl. Acad. Sci. U.S.A. 115 (2018) 10983–10988.
[10] S. Taghvaei, F. Sabouni, Z. Minuchehr, Evidence of omics, immune infiltration, and pharmacogenomic for SENP1 in the pan-cancer cohort, Front. Pharmacol. 12 (2021) 700454.
[11] L. Sun, H. Zhang, P. Gao, Metabolic reprogramming and epigenetic modifications on the path to cancer, Protein & Cell 13 (2022) 877–919.
[12] T. Ge, X. Gu, R. Jia, et al., Crosstalk between metabolic reprogramming and epigenetics in cancer: updates on mechanisms and therapeutic opportunities, Cancer Commun. 42 (2022) 1049–1082.
[13] Y. Gong, P. Ji, Y.-S. Yang, et al., Metabolic-pathway-based subtyping of triple-negative breast cancer reveals potential therapeutic targets, Cell Metabol. 33 (2021).
[14] Y. Vivas-García, P. Falletta, J. Liebing, et al., Lineage-restricted regulation of SCD and fatty acid saturation by MITF controls melanoma phenotypic plasticity, Mol. Cell 77 (2020).
[15] T.-J. Yu, D. Ma, Y.-Y. Liu, et al., Bulk and single-cell transcriptome profiling reveal the metabolic heterogeneity in human breast cancers, Mol. Ther. : the Journal of the American Society of Gene Therapy 29 (2021) 2350–2365.
[16] C. Sun, T. Li, X. Song, et al., Spatially resolved metabolomics to discover tumor-associated metabolic alterations, Proc. Natl. Acad. Sci. U.S.A. 116 (2019) 52–57.
[17] Q. Liang, Q. Zheng, Y. Zuo, et al., SENP2 suppresses Necdin expression to promote Brown adipocyte differentiation, Cell Rep. 28 (2019).
[18] Q. Zheng, Y. Cao, Y. Chen, et al., Senp2 regulates adipose lipid storage by de-SUMOylation of Setdb1, J. Mol. Cell Biol. 10 (2018) 258–266.
[19] Y.D. Koo, J.S. Lee, S.-A. Lee, et al., SUMO-specific protease 2 mediates leptin-induced fatty acid oxidation in skeletal muscle, Metab., Clin. Exp. 95 (2019) 27–35.
[20] B. Eymin, Inspiratory hyperoxia: a new way to prevent metastasis through metabolism reprogramming in non-small cell lung cancer, Eur. Respir. J. 60 (2022).
[21] J. Sun, J. Ding, Q. Shen, et al., Decreased propionyl-CoA metabolism facilitates metabolic reprogramming and promotes hepatocellular carcinoma, J. Hepatol. (2022).
[22] J. Liu, Z.-X. Liu, Q.-N. Wu, et al., Long noncoding RNA AGPG regulates PFKFB3-mediated tumor glycolytic reprogramming, Nat. Commun. 11 (2020) 1507.
[23] P. Yang, H. Qin, Y. Li, et al., CD36-mediated metabolic crosstalk between tumor cells and macrophages affects liver metastasis, Nat. Commun. 13 (2022) 5782.
[24] H. Yang, Q. Deng, T. Ni, et al., Targeted Inhibition of LPL/FABP4/CPT1 fatty acid metabolic axis can effectively prevent the progression of nonalcoholic steatohepatitis to liver cancer, Int. J. Biol. Sci. 17 (2021) 4207–4222.
[25] T. Yoshida, T. Yokobori, H. Saito, et al., CD36 expression is associated with cancer aggressiveness and energy source in esophageal squamous cell carcinoma, Ann. Surg Oncol. 28 (2021) 1217–1227.
[26] M.-Y. Cui, X. Yi, D.-X. Zhu, et al., Identification of differentially expressed genes related to the lipid metabolism of esophageal squamous cell carcinoma by integrated bioinformatics analysis, Curr. Oncol. 30 (2022).
[27] T. Tian, Y. Lu, J. Lin, et al., CPT1A promotes anoikis resistance in esophageal squamous cell carcinoma via redox homeostasis, Redox Biol. 58 (2022) 102544.
[28] Y. Liu, X. Dou, W.-Y. Zhou, et al., Hepatic small ubiquitin-related modifier (SUMO)-Specific protease 2 controls systemic metabolism through SUMOylation-dependent regulation of liver-adipose tissue crosstalk, Hepatology 74 (2021) 1864–1883.
[29] M. Mazumder, P. Ponnan, U. Das, et al., Investigations on binding pattern of kinase inhibitors with PPARγ: molecular docking, molecular dynamic simulations, and free energy calculation studies, PPAR Res. 2017 (2017) 6397836.
[30] S.S. Chung, B.Y. Ahn, M. Kim, et al., SUMO modification selectively regulates transcriptional activity of peroxisome-proliferator-activated receptor γ in C2C12 myotubes, Biochem. J. 433 (2011) 155–161.
[31] Y.D. Koo, J.W. Choi, M. Kim, et al., SUMO-specific protease 2 (SENP2) is an important regulator of fatty acid metabolism in skeletal muscle, Diabetes 64 (2015) 2420–2431.
[32] L. Maréchal, M. Laviolette, A. Rodrigue-Way, et al., The CD36-PPARγ pathway in metabolic disorders, Int. J. Mol. Sci. 19 (2018).

[33] F. Zhao, C. Xiao, K.S. Evans, et al., Paracrine Wnt5a-β-catenin signaling triggers a metabolic program that drives dendritic cell tolerization, Immunity 48 (2018).
[34] J. Padeken, S.P. Methot, S.M. Gasser, Establishment of H3K9-methylated heterochromatin and its functions in tissue differentiation and maintenance, Nat. Rev. Mol. Cell Biol. 23 (2022) 623–640.
[35] L. Sun, J. Fang, E3-Independent constitutive monoubiquitination complements histone methyltransferase activity of SETDB1, Mol. Cell 62 (2016) 958–966.